Journal of Engineering Mathematics **27:** 161–188, 1993.

The effect of a uniform magnetic field on the onset of steady Bénard-Marangoni convection in a layer of conducting fluid

S. K. WILSON
Department of Mathematics, University of Strathclyde, Livingstone Tower, 26 Richmond Street, Glasgow G1 1XH, United Kingdom

Received 15 February 1992; accepted in revised form 21 July 1992

Abstract. In this paper we use a combination of analytical and numerical techniques to analyse the effect of a uniform vertical magnetic field on the onset of steady Bénard-Marangoni convection in a horizontal layer of quiescent, electrically conducting fluid subject to a uniform vertical temperature gradient. The critical values of the Rayleigh and Marangoni numbers for the onset of steady convection are calculated and the latter is found to be critically dependent on the non-dimensional Crispation and Bond numbers. The stability of the layer to long wavelength disturbances is analysed and the two different asymptotic limits of strong surface tension (small Crispation number) and strong magnetic field (large Chandrasekhar number) are investigated. In the latter case analytical results for the critical Rayleigh and Marangoni numbers are obtained and are found to be in excellent agreement with the results of numerical calculations. We conclude that the presence of the magnetic field always has a stabilising effect on the layer. Treating the Marangoni number as the critical parameter we show that if the free surface is non-deformable then any particular disturbance can be stabilised with a sufficiently strong magnetic field, but if the free surface is deformable and gravity waves are excluded then the layer is always unstable to infinitely long wavelength disturbances with or without a magnetic field. Including gravity has a stabilising effect on the long wavelength modes, but not all disturbances can be stabilised no matter now strong the magnetic field is.

1. Introduction

The aim of this paper is to investigate the effect of a uniform vertical magnetic field on the Bénard-Marangoni instability of a horizontal three dimensional planar layer of quiescent electrically conducting fluid, subject to a uniform vertical temperature gradient.

The classical buoyancy-driven instability of a horizontal fluid layer heated from below has received considerable attention since the pioneering work of Rayleigh [1], who showed that steady convection (often called Bénard convection) occurs only when the *Rayleigh number*, R, defined as

$$R = \frac{g\alpha(T_1 - T_2)d^3}{\nu\kappa},$$

exceeds a critical value, where g is the acceleration due to gravity, α is the coefficient of volume expansion, T_1 is the constant temperature of the lower solid boundary, T_2 is the constant temperature of the upper free surface, d is the thickness of the layer, ν is the kinematic viscosity and κ the thermal diffusivity of the fluid. Rayleigh's [1] work was restricted to the limit of large surface tension and later Pellew & Southwell [2] proved that in this case instability must always set in as steady, rather than overstable, convection. Recently Benguria & Depassier [3] have found overstable convection when the free surface is allowed to deform.

In his pioneering contribution Pearson [4] showed that, even in the absence of buoyancy forces, a thermocapillary force at the free surface caused by the dependence of the surface tension on temperature causes steady convection (usually called Marangoni convection) to occur in a fluid layer heated from below provided that the *Marangoni number*, M, defined as

$$M = \frac{\gamma(T_1 - T_2)d}{\rho_0 \nu \kappa},$$

exceeds a critical value, where the constant $-\gamma$ is the rate of change of surface tension with respect to temperature and ρ_0 is the density of the fluid. Pearson's [4] work was also restricted to the limit of large surface tension, but subsequently Scriven & Sterling [5], Smith [6] and Takashima [7] showed that similar behaviour occurs when the free surface is allowed to deform. Takashima [8, 9] showed numerically that overstable Marangoni convection can also occur, but only if the layer is heated from above $(M < 0)$ and the free surface is allowed to deform.

The combined problem including both buoyancy and thermocapillary effects was treated by Nield [10] in the limit of large surface tension who found that for steady convection the two destabilising mechanisms are tightly coupled and reinforce one another. Davis & Homsy [11] studied the effect of free surface deformation on the combined problem and concluded that surface deflection *stabilizes* buoyancy dominated convection and *destabilizes* surface tension dominated convection. Oscillatory instabilities for the combined problem have recently been found by Benguria & Depassier [12] and Gouesbert et al. [13], but again only if the free surface is allowed to deform.

The effect of a uniform vertical magnetic field on pure buoyancy-driven convection was described by Chandrasekhar [14] who demonstrated that the effect of including the field is to increase the critical value of R for the onset of both steady and overstable convection, and hence to have a stabilising effect on the layer. Nield [15] analysed the effect of a magnetic field on the combined problem for steady convection in the limit of large surface tension and showed that, although the tight coupling between two destabilising mechanisms was weakened, the effect of increasing the strength of the field from zero was to monotonically increase the critical values of R and M and hence to stabilise the layer. More recently this limit was also investigated by Maekawa & Tanasawa [16, 17]. In a series of papers Sarma investigated the effect of a magnetic field on the onset of steady convection when the free surface is allowed to deform in both the purely surface tension-driven [18, 19] and combined [20, 21, 22, 23] problems for a variety of thermal and magnetic boundary conditions. Unfortunately he used an incorrect normal stress boundary condition in his analysis and so his results in the case of a non-zero magnetic field and a deformable free surface must be reviewed. Wilson [24] used the correct normal stress boundary condition to describe the onset of steady Marangoni convection and showed that, although the effect of the magnetic field is always a stabilising one, an arbitrarily large magnetic field cannot stabilise all disturbances. Wilson [24] also demonstrated that the presence of a magnetic field also has a stabilising effect on the onset of overstable Marangoni convection.

The purpose of the present work is to investigate the effect of a magnetic field on the onset of steady Bénard-Marangoni convection in a planar layer heated from below, and to do this we extend the approach taken by Wilson [24] to include buoyancy effects. In the case of a non-deformable free surface we give numerically calculated values of the critical parameters which extend and correct those of Nield [15] and Maekawa & Tanasawa [16, 17] and give the correct description of the behaviour in the limiting case of a strong magnetic field. In the case of a deformable free surface we recalculate the results of Davis & Homsy [11] in the limit of strong surface tension for the non-magnetic problem and give the corresponding results in the presence of a magnetic field. Finally, we give illustrative numerically calculated values of the critical parameters for a particular choice of parameter values.

2. Problem formulation

The basic geometry we wish to examine is that of an unbounded horizontal layer of quiescent fluid of thickness d subject to a uniform vertical magnetic field of strength H and a uniform vertical temperature gradient. The layer of fluid is bounded below by a horizontal planar solid boundary at constant temperature T_1, and above by a free surface at constant temperature T_2 which is in contact with a passive gas at constant pressure P_0 and constant temperature T_∞. The fluid is assumed to have constant, non-zero electrical resistivity. We choose rectangular axes with the x - and y -axes in the plane of the lower solid boundary and the z -axis vertically upwards, so that the lower boundary is given by $z = 0$ and in the undisturbed state the free surface is located at $z = d$. When motion occurs the free surface will be deformed and then we denote its position by $z = d + f(x, y, t)$. The surface tension of the free surface, τ, is assumed to be dependent on temperature T according to the simple linear law,

$$\tau = \tau_0 - \gamma (T - T_0),$$

where τ_0 is the value of τ at the suitably chosen reference temperature T_0 and the constant γ is positive for normal fluids.

Subject to the Boussinesq approximation the governing equations for an incompressible, electrically conducting fluid in the presence of a magnetic field are

$$\frac{\partial \mathbf{U}}{\partial t} + (\mathbf{U} \cdot \nabla) \mathbf{U} = -\frac{1}{\rho_0} \nabla \Pi + \nu \nabla^2 \mathbf{U} + \frac{\rho}{\rho_0} \mathbf{g} + \frac{\mu}{4\pi\rho_0} (\mathbf{H} \cdot \nabla) \mathbf{H}, \quad (1)$$

$$\frac{\partial \mathbf{H}}{\partial t} + (\mathbf{U} \cdot \nabla) \mathbf{H} = (\mathbf{H} \cdot \nabla) \mathbf{U} + \eta \nabla^2 \mathbf{H}, \quad (2)$$

$$\frac{\partial T}{\partial t} + \mathbf{U} \cdot \nabla T = \kappa \nabla^2 T, \quad (3)$$

$$\nabla \cdot \mathbf{U} = 0, \quad (4)$$

$$\nabla \cdot \mathbf{H} = 0, \quad (5)$$

where $\mathbf{U}$ is the fluid velocity, $\mathbf{H}$ is the magnetic field, T is the temperature, $\mathbf{g} = (0, 0, -g)$ is the external gravity field and Π is the magnetic pressure, which is defined to be $\Pi = P + \mu|\mathbf{H}|^2/8\pi$ where P is the fluid pressure. The density of the fluid is given by

$$\rho = \rho_0 \{1 - \alpha(T - T_0)\},$$

where α is the coefficient of volume expansion and the constant ρ_0 is the value of the density at the reference temperature T_0. The other properties of the fluid are represented by the kinematic viscosity ν, the magnetic permeability μ, the electrical conductivity $\bar{\sigma}$, the electrical resistivity $\eta = 1/4\pi\mu\bar{\sigma}$ and the thermal diffusivity κ. At the free surface we have the usual kinematic condition together with conditions of continuity of the normal and

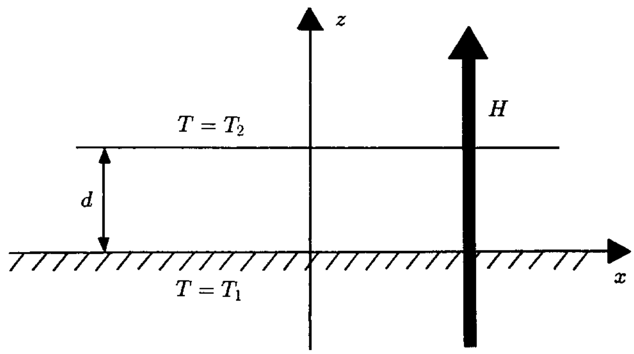

Fig. 1. Geometry of the unperturbed state.

tangential stresses, and for the temperature Newton's law of cooling,

$$-k\frac{\partial T}{\partial \mathbf{n}} = h(T - T_\infty),$$

where k is the thermal conductivity of the fluid, h is the heat transfer coefficient between the free surface and the gas and $\mathbf{n}$ is the outward unit normal to the free surface. At the fixed lower boundary the usual no-slip condition requires continuity of velocity between the solid and the fluid, and the temperature takes the constant value T_1. We also require boundary conditions for the magnetic field but, as we shall see, in the special case of the onset of steady convection we can eliminate the magnetic field entirely from the problem and so do not need to specify them in the present work.

If we identify the reference temperature T_0 with T_2, the temperature of the free surface in the undisturbed state, then there is a basic state in which the fluid is at rest $\mathbf{U} \equiv \mathbf{0}$, the magnetic field is uniform, $\mathbf{H} = (0, 0, H)$, the free surface is flat, $f(x, y, t) = 0$, there is a uniform temperature gradient across the layer, $T = T_1 - (T_1 - T_2)z/d$, where $T_1 - T_2 = (T_2 - T_\infty)hd/k$ and the pressure is given by

$$P = P_0 - \rho_0 g(z - d)\left[1 + \frac{\alpha(T_1 - T_2)}{2d}(z - d)\right].$$

The geometry of the basic state is shown in Fig. 1 and in what follows we shall investigate the linear stability of perturbations to this basic state.

3. Non-dimensionalisation

To simplify the analysis we introduce non-dimensional variables. Taking d as the unit of length, appropriate scales for the velocity, magnetic field, temperature gradient and time are κ/d, H, $(T_1 - T_2)/d$ and d^2/κ respectively. Non-dimensionalising the equations and boundary conditions gives rise to eight non-dimensional groups which, in addition to the *Rayleigh number*, R, and the *Marangoni number*, M, defined above, are the *Prandtl number*, $P_r = \nu/\kappa$, the *Magnetic Prandtl number*, $P_m = \eta/\kappa$, the *Chandrasekhar number*, $Q = \mu H^2 d^2/4\pi\rho_0\nu\eta$, the *Crispation number*, $C_r = \rho_0\nu\kappa/\tau_0 d$, the *Nusselt (or Biot) number*, $N_u = hd/k$, and the *Bond number*, $B_o = \rho_0 g d^2/\tau_0$.

4. The linearised problem

We analyse the linear stability of the basic state in the usual manner by seeking perturbed solutions for any quantity $\Phi(x, y, z, t)$ in the form

$$\Phi(x, y, z, t) = \Phi_0(x, y, z) + \phi(z) e^{\sigma t} e^{i(\alpha x + \beta y)},$$

where Φ_0 is the value of Φ in the basic state and the temporal exponent σ will, in general, be complex. Substituting these forms of solution into equations (1), (2) and (3) and neglecting second order and higher terms in the perturbed quantities we obtain the corresponding linearised equations, which can be combined into three equations using equations (4) and (5). In the present work we shall treat only the onset of steady convection and so set $\sigma = 0$ in the equations and boundary conditions. In this special case we can eliminate the magnetic field and the parameters P_r and P_m from the problem by combining the linearised versions of equations (1) and (2) to obtain two linear equations involving only the $z-$dependent part of the $z-$component of the perturbation to the velocity, denoted by $w(z)$, and the $z-$dependent part of the perturbation to the temperature, denoted by $T(z)$:

$$\left[(D^2 - a^2)^2 - QD^2\right] w - a^2 RT = 0, \tag{6}$$

$$(D^2 - a^2)T + w = 0. \tag{7}$$

The operator $D = \mathrm{d}/\mathrm{d}z$ denotes differentiation with respect to z and the quantity $a = (\alpha^2 + \beta^2)^{1/2}$ is the total wave number in the x-y plane. When $\sigma = 0$ the linearised versions of the boundary conditions at the free surface become

$$w = 0, \tag{8}$$

$$C_r(D^2 - 3a^2 - Q)Dw - a^2(a^2 + B_o)f = 0, \tag{9}$$

$$(D^2 + a^2)w + a^2 M(T - f) = 0, \tag{10}$$

$$DT + N_u(T - f) = 0, \tag{11}$$

evaluated on $z = 1$, while at the solid boundary we have

$$w = 0, \tag{12}$$

$$Dw = 0, \tag{13}$$

$$T = 0, \tag{14}$$

evaluated on $z = 0$. Notice that, even though the magnetic field has been eliminated from the governing equations and boundary conditions, magnetic field effects are still included via the Chandrasekhar number Q. This problem was investigated by Sarma [18, 19, 20, 21, 22, 23] who incorrectly omitted the term due to the magnetic field in the normal stress boundary condition (9).

To solve the linearised problem for the onset of steady convection we seek solutions in the forms

$$w(z) = ACe^{\xi z}, \quad T(z) = Ce^{\xi z},$$

where the exponent ξ and the complex quantities A and C are to be determined. Substituting these forms into the equations (6) and (7) and eliminating A and C we obtain a sixth order algebraic equation for ξ, namely

$$(\xi^2 - a^2)\left[(\xi^2 - a^2)^2 - Q\xi^2\right] + a^2 R = 0, \tag{15}$$

with six distinct roots, which we denote by $\xi_1, \ldots, \xi_6$. Denoting the values of A and C corresponding to ξ_i for $i = 1, \ldots, 6$ by A_i and C_i we can use equation (7) to determine A_i to be $A_i = -\left(\xi_i^2 - a^2\right)$ for $i = 1, \ldots, 6$. We can use equation (9) to eliminate the free surface deflection

$$f = \frac{C_r\left(D^2 - 3a^2 - Q\right)Dw}{a^2(a^2 + B_o)}$$

evaluated on $z = 1$, which leaves the six boundary conditions (8), (10), (11), (12), (13) and (14) to determine the six unknowns $C_1, \ldots, C_6$ (up to an arbitrary multiplier). The dispersion relation between M, R, a, C_r, Q, B_o and N_u is determined by substituting the solutions for $w(z)$ and $T(z)$ into the boundary conditions and evaluating the resulting 6×6 complex determinant of the coefficients of the unknowns, which can be written in the form

$$D_1 + MD_2 = 0,$$

where the two 6×6 complex determinants D_1 and D_2 can depend on all the parameters of the problem except for M. After some simplification the elements of the determinant $D_1 = |d_{ij}|$ are given by

$$d_{1i} = A_i e^{\xi_i}, \tag{16}$$

$$d_{2i} = \xi_i^2 A_i e^{\xi_i}, \tag{17}$$

$$d_{3i} = (\xi_i + N_u)\, e^{\xi_i}, \tag{18}$$

$$d_{4i} = A_i, \tag{19}$$

$$d_{5i} = \xi_i A_i, \tag{20}$$

$$d_{6i} = 1 \tag{21}$$

for $i = 1, \ldots, 6$. The coefficients of the determinant D_2 are the same as those of D_1 apart from the terms

$$d_{2i} = a^2\left[1 - \frac{C_r\left(\xi_i^2 - 3a^2 - Q\right)\xi_i A_i}{a^2(a^2 + B_o)}\right] e^{\xi_i}, \tag{22}$$

$$d_{3i} = \xi_i e^{\xi_i} \tag{23}$$

for $i = 1, \ldots, 6$. Notice that D_1 is independent of C_r and B_o and that D_2 is independent of N_u. One immediate consequence of this is that the onset of steady Bénard convection ($M = 0$) is independent of C_r and B_o, and so the results obtained by Chandrasekhar [14] in the case $C_r = 0$ also apply to the more general problem with $C_r \neq 0$ when the free surface is deformable.

The method of solution described above gives, in principal, the complete solution for the linear stability problem. In practice, however, we have to turn to numerical computation in order to evaluate the complex determinants D_1 and D_2 and to determine the marginal stability curves. In order to the prevent numerical difficulties arising from the exponential terms the i th columns of D_1 and D_2 were both multiplied by an exponential factor with exponent $\min(0, -Re(\xi_i))$, where $Re(\cdot)$ denotes the real part of a complex quantity, and then evaluated using NAG routine F03ADF.

5. Results

On the marginal stability curves in the (a, M) plane $M = M(a, R, C_r, Q, B_o, N_u)$ and the region *above* the marginal stability curve represents unstable modes and the region *below* the curve represents stable modes, and so for a given set of parameters the *critical Marangoni number for the onset of steady convection* is defined to be the global minimum of the corresponding marginal stability curve. We denote this critical value by $M_c = M_c(R, C_r, Q, B_o, N_u)$ and the corresponding critical wave number by $a_c = a_c(R, C_r, Q, B_o, N_u)$, and so for $M < M_c$ all disturbances are stable and for $M > M_c$ unstable disturbances exist. In Appendix A we show that on the marginal stability curves $M \sim 8a^2$ as $a \to \infty$ regardless of the values of the other parameters. If $C_r = 0$ then $M = O(1/a^2)$ for $a \ll 1$ and the curves always have their global minimum at a non-zero value of a. In the simplest case $Q = 0$, $R = 0$ we recover Pearson's [4] critical value of $M_c = 79.607$ at $a_c = 1.99$ when $N_u = 0$ and find that $M_c/N_u \sim 32.073$ at $a_c = 3.01$ in the limit $N_u \to \infty$. If $C_r \neq 0$ but $B_o = 0$ then

$$M \sim \frac{a^2}{C_r} g(Q^{1/2})(1 + N_u) \tag{24}$$

for $a \ll 1$ and so $M_c = 0$ at $a_c = 0$, while if $C_r \neq 0$ and $B_o \neq 0$ then

$$M \sim \frac{B_o}{C_r} g(Q^{1/2})(1 + N_u) \tag{25}$$

for $a \ll 1$ and M_c can occur either at a non-zero value of a_c or at $a_c = 0$ depending where the *global* minimum occurs. In the above we have defined the function

$$g(H) = \frac{\sinh H - H \cosh H}{H(1 - \cosh H)}, \tag{26}$$

which is plotted in Fig. 2. Notice that $g(H) \to 2/3$ as $H \to 0$ and so we recover the corresponding results for the problem without a magnetic field given by Takashima [7] while $g(H) \to 1$ as $H \to \infty$. Since the parameter R only occurs in the problem multiplied by the factor a^2 these leading order expressions for M when $a \ll 1$ are exactly the same as those obtained by Wilson [24] in the case $R = 0$.

On the marginal stability curves in the (a, R) plane $R = R(a, M, C_r, Q, B_o, N_u)$ and again the region *above* the marginal stability curve represents unstable modes and the region *below* the curve represents stable modes, and so for a given set of parameters the *critical Rayleigh number for the onset of steady convection* is defined to be the global minimum of the corresponding marginal stability curve. We denote this critical value by $R_c = R_c(M, C_r, Q, B_o, N_u)$

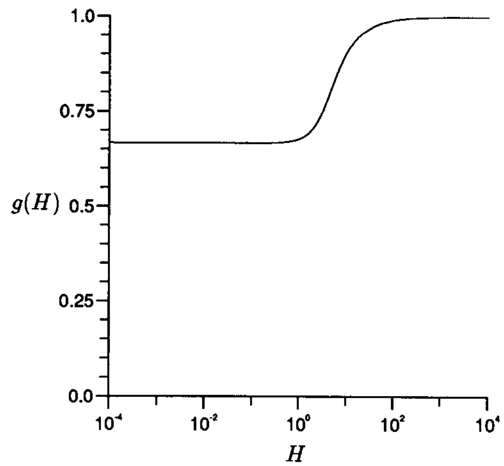

Fig. 2. The function $g(\cdot)$ given by equation (28).

and the corresponding critical wave number by $a_c = a_c(M, C_r, Q, B_o, N_u)$, and so for $R < R_c$ all disturbances are stable and for $R > R_c$ unstable disturbances exist. The behaviour of these curves is rather harder to determine, but in the case of pure buoyancy-driven convection $M = 0$ then $R = O(1/a^2)$ for $a \ll 1$ and $R = O(a^4)$ as $a \to \infty$ and there is a single global minimum value of R at a non-zero value of a. When in addition $Q = 0$ we recover the well-known values of $R_c = 669.00$ at $a_c = 2.086$ when $N_u = 0$ and $R_c = 1100.65$ at $a_c = 2.682$ in the limit $N_u \to \infty$.

Of course, what we really need for the combined problem is the marginal stability *surface* in three-dimensional (a, M, R) space separating the region of unstable modes from the region of stable modes. However, because of the particularly simple way in which the parameter M occurs in the problem it is usually convenient to work with M as the critical parameter for a range of values of R.

5.1. Non-deformable free surface $C_r = 0$

In practice the value of C_r may be very small (for a 1 cm layer of water open to air at 20^o C we have $C_r \sim 10^{-7}$) and so perhaps the most obvious simplification to make is to consider the limit of large surface tension, $C_r = 0$, in which the free surface is non-deformable.

Table 1 gives the numerically calculated values of R_c and M_c with the corresponding values of a_c for purely buoyancy-driven and purely thermocapillary-driven convection respectively in the case $N_u = 0$ and the limit $N_u \to \infty$ when $C_r = 0$. It extends and corrects the similar results given by Nield [15] and Maekawa & Tanasawa [16,17] by giving more accurate values over a larger range of values of Q.

The conditions for the onset of steady convection in this case were fairly completely described by Nield [15] and are illustrated in Fig. 3 and Fig. 4, which show M_c^* and a_c in the case $N_u = 0$ together with M_c^*/N_u and a_c in the limit $N_u \to \infty$ plotted as functions of R^*, where R^* is defined to be the value of R divided by the corresponding value of R_c for pure buoyancy-driven convection and M^* is defined to be the value of M divided by the corresponding value of M_c for pure thermocapillary-driven convection. As Nield [15] demonstrated when $M > 0$, $R > 0$ and $Q = 0$ the two destabilising mechanisms are tightly

Table 1. Numerically calculated values of R_c and M_c and the corresponding values of a_c for pure buoyancy-driven and pure thermocapillary-driven convection respectively when $C_r = 0$ in the case $N_u = 0$ and the limit $N_u \to \infty$ for a range of values of Q. In the latter case the limiting value of M_c/N_u rather than M_c is given.

		$N_u = 0$		
Q	R_c	a_c	M_c	a_c
10^{-4}	669.0004	2.0856	79.60696	1.9929
10^{-3}	669.0197	2.0856	79.60928	1.9929
10^{-2}	669.2130	2.0859	79.63249	1.9931
10^{-1}	671.1453	2.0880	79.86452	1.9951
1	690.3729	2.1091	82.17241	2.0147
10	874.8618	2.2884	104.2227	2.1810
10^2	2424.903	3.1281	284.2223	2.9589
10^3	14594.63	4.9910	1632.472	4.7448
10^4	118360.3	7.9486	12830.16	8.0924
10^5	1074679.	12.2337	114212.7	14.1872
10^6	1.0270543×10^7	18.4202	1075322.	25.1160
10^7	1.0054710×10^8	27.4234	1.0410180×10^7	44.6003
10^8	9.9554189×10^8	40.5868	–	–
		$N_u \to \infty$		
Q	R_c	a_c	M_c/N_u	a_c
10^{-4}	1100.652	2.6823	32.07307	3.0141
10^{-3}	1100.677	2.6824	32.07366	3.0141
10^{-2}	1100.920	2.6826	32.07961	3.0145
10^{-1}	1103.351	2.6851	32.13898	3.0183
1	1127.498	2.7099	32.06755	3.0553
10	1355.487	2.9186	38.06755	3.3804
10^2	3149.559	3.8500	71.98895	5.1982
10^3	16117.90	5.7486	210.6965	12.4993
10^4	122138.3	8.6358	666.0381	39.3076
10^5	1085076.	12.8481	2106.198	124.3014
10^6	1.0301066×10^7	18.9886	6660.381	393.0757
10^7	1.0063990×10^8	27.9651	21061.97	1243.015
10^8	9.9582931×10^8	41.1129	66603.81	3930.757

coupled and reinforce each other. As Q is increased from zero this coupling is progressively weakened, but the effect of the magnetic field is to cause a monotonic increase in M_c and R_c viewed as functions of Q, and hence is always a stabilising influence on the system. As Q becomes large the marginal stability curves may develop more than one local minimum which results in the discontinuity in the graph of a_c as a function of R shown in Fig. 4(b) produced as the absolute values at two different local minima vary and the position of the global minimum jumps discontinuously from one to the other.

The limit $Q \to \infty$

The numerical calculations indicate that in the limit $Q \to \infty$ the values of R_c and M_c each approach the same limits as they do in the absence of the other destabilising mechanism.

In Appendix B we show that for pure Bénard convection the limiting values of R_c and a_c as $Q \to \infty$ are

$$R_c = \pi^2 Q + 3\left(\frac{\pi^4}{2}\right)^{2/3} Q^{2/3} + o\left(Q^{2/3}\right) \tag{27}$$

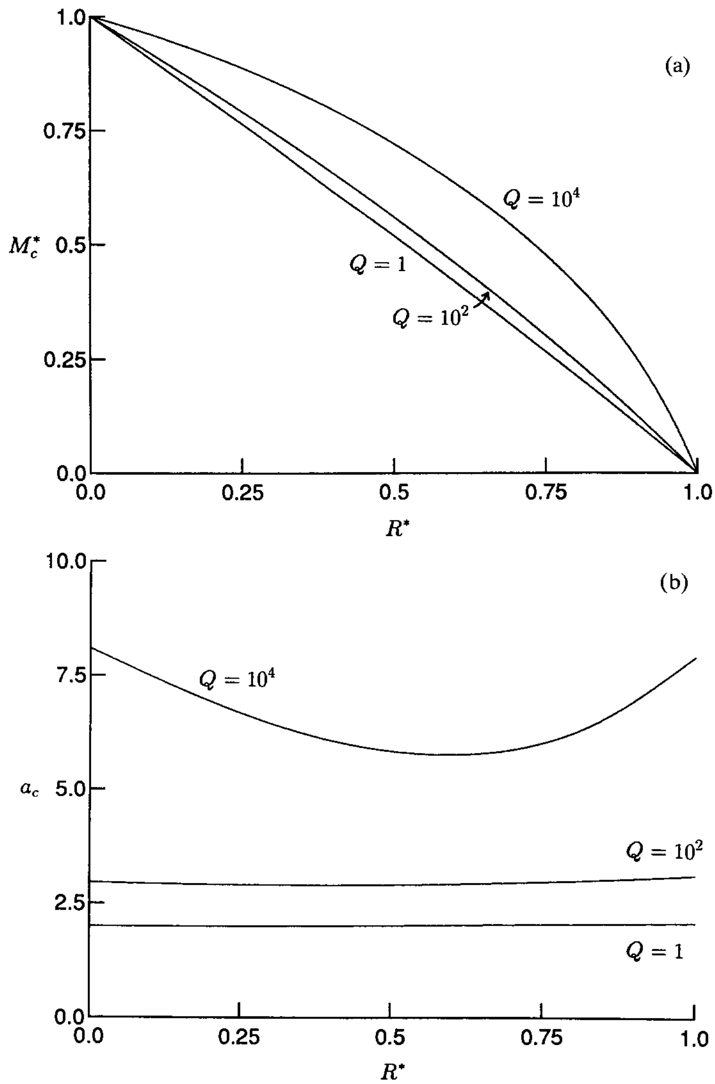

Fig. 3. Critical conditions for the onset of stationary convection in the case $C_r = 0$ and $N_u = 0$ plotted as functions of R^* for $Q = 1$, 10^2 and 10^4 (a) M_c^* (b) a_c.

and

$$a_c = \left(\frac{\pi^4}{2}\right)^{1/6} Q^{1/6} + o\left(Q^{1/6}\right). \tag{28}$$

Figure 5 shows the numerically calculated values of R_c/Q, $(R_c - \pi^2 Q)/Q^{2/3}$ and $a_c/Q^{1/6}$ plotted as functions of Q for different values of N_u and verifies that $R_c/Q \to \pi^2 \approx 9.869604401$, $(R_c - \pi^2 Q)/Q^{2/3} \to 3\left(\pi^4/2\right)^{2/3} \approx 40.00991095$ and $a_c/Q^{1/6} \to (\pi^4/2)^{1/6} \approx 1.91100394$ as $Q \to \infty$ as predicted.

In Appendix C we extend the method of Wilson [24] to show that for pure Marangoni convection the limiting values of M_c and a_c as $Q \to \infty$ are

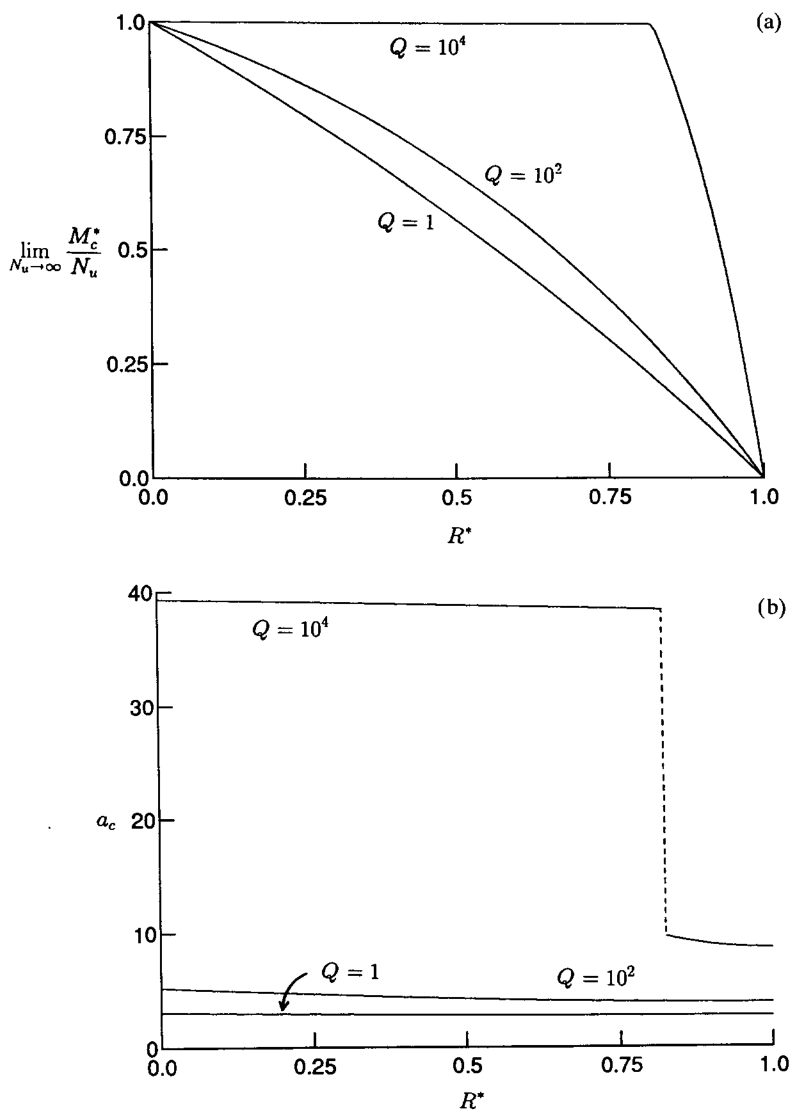

Fig. 4. Critical conditions for the onset of stationary convection in the case $C_r = 0$ and $N_u \to \infty$ plotted as functions of R^* for $Q = 1$, 10^2 and 10^4 (a) $\lim_{N_u \to \infty} M_c^*/N_u$ (b) a_c.

$$M_c = Q + f_1(\hat{a})Q^{3/4} + o\left(Q^{3/4}\right) \tag{29}$$

and

$$a_c = \hat{a}Q^{1/4} + o\left(Q^{1/4}\right), \tag{30}$$

where we have defined the function

$$f_1(\hat{a}) = \frac{2\hat{a}}{\left(1 - e^{-2\hat{a}^2}\right)} + \frac{N_u}{\hat{a}}, \tag{31}$$

and the coefficient $\hat{a}$ is determined by the equation $\mathrm{d}f_1/\mathrm{d}\hat{a} = 0$. This equation can easily be solved numerically and the values of $\hat{a}$ and $f_1(\hat{a})$ are given in Table 2 for a range of

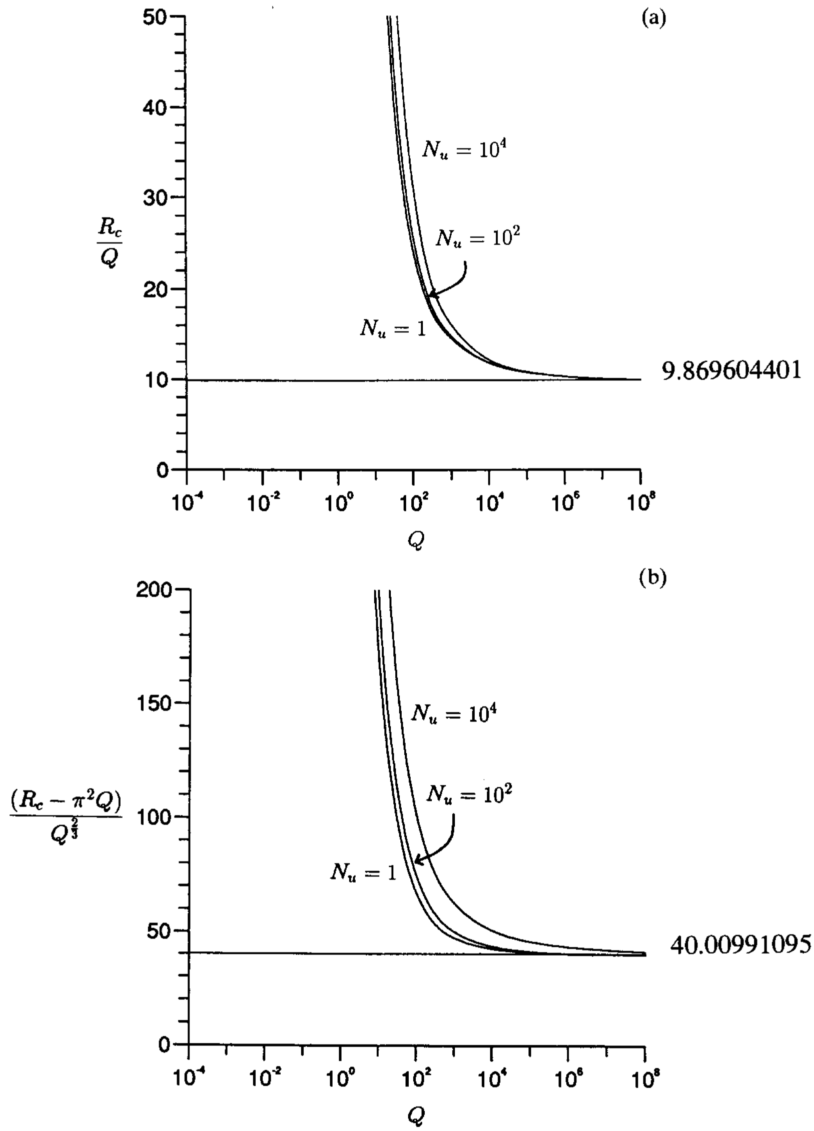

Fig. 5. Comparison of numerically calculated and asymptotic results for pure buoyancy-driven convection in the limit $Q \to \infty$ plotted as functions of Q when $C_r = 0$ for $N_u = 1$, 10^2 and 10^4 (a) R_c/Q (b) $(R_c - \pi^2 Q)/Q^{2/3}$ (c) $a_c/Q^{1/6}$.

values of N_u. Fig. 6 shows the numerically computed values of M_c/Q, $(M_c - Q)/Q^{3/4}$ and $a_c/Q^{1/4}$ plotted as functions of Q for different values of N_u and verifies the values of the asymptotic limits given in Table 2. In the special case $N_u \to \infty$ Wilson [24] showed that the limiting values of M_c/N_u and a_c as $Q \to \infty$ are

$$\frac{M_c}{N_u} = f_2(\hat{a})Q^{1/2} + o\left(Q^{1/2}\right) \tag{32}$$

and

$$a_c = \hat{a}Q^{1/2} + o(Q^{1/2}), \tag{33}$$

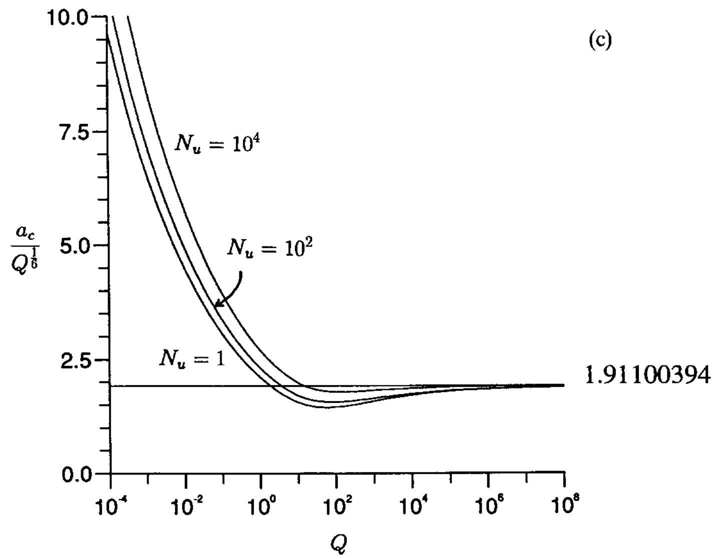

Fig. 5 (c).

where we have defined the function

$$f_2(\hat{a}) = \frac{1}{\hat{a}}\left[1 - \frac{2\hat{a}}{(1+4\hat{a}^2)^{1/2}}\right]^{-1}, \tag{34}$$

and the coefficient $\hat{a}$ is determined by the equation $\mathrm{d}f_2/\mathrm{d}\hat{a} = 0$. This equation can easily be solved numerically to yield the solution $\hat{a} \approx 0.39307569$ with the corresponding value $f_2(\hat{a}) \approx 6.66038135$.

Table 2. Numerically calculated values of $\hat{a}$ and the corresponding values of $f_1(\hat{a})$ obtained by solving the equation $\mathrm{d}f_1/\mathrm{d}\hat{a} = 0$ for a range of values of N_u.

N_u	$\hat{a}$	$f_1(\hat{a})$
0	0.79260053	2.2160358672
1	1.02652433	3.3112632065
2	1.19905121	4.2094005590
3	1.34843714	4.9946370376
4	1.48768362	5.7001191814
5	1.62212906	6.3435255358
10	2.23702573	8.9444741278
15	2.73862493	10.9544528255
20	3.16227779	12.6491106537
25	3.53553391	14.1421356238
50	5.00000000	20.0000000000
100	7.07106781	28.2842712475

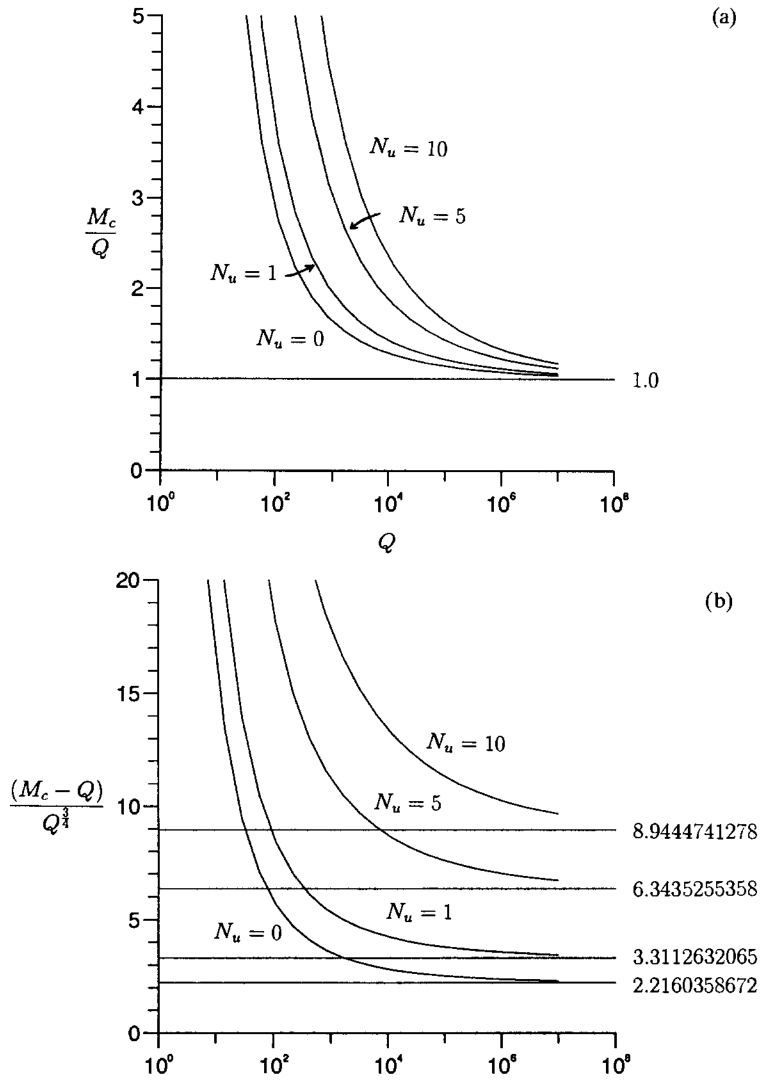

Fig. 6. Comparison of numerically calculated and asymptotic results for pure thermocapillary-driven convection in the limit $Q \to \infty$ plotted as functions of Q when $C_r = 0$ for $N_u = 0, 1, 5$ and 10 (a) M_c/Q (b) $(M_c - Q)/Q^{3/4}$ (c) $a_c/Q^{1/4}$.

5.2. Deformable Free Surface $C_r \neq 0$

While in practice the value of C_r may indeed be very small it will inevitably be non-zero and, as we have already seen, if the free surface is allowed to deform ($C_r \neq 0$) then the marginal stability curves differ fundamentally from those in the case $C_r = 0$ in the region $a \ll 1$ and depend critically on whether B_o is zero or not. However, before we consider this singular behaviour we shall investigate the regular behaviour in the limit $C_r \to 0$ away from $a = 0$.

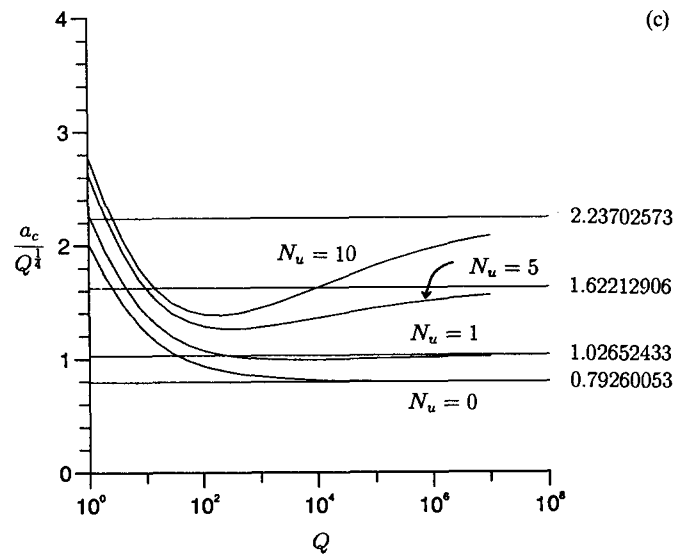

Fig. 6 (c).

The limit $C_r \to 0$

Following Davis & Homsy [11], who investigated the problem without a magnetic field, we analyse the effect of small, non-zero values of C_r by seeking solutions for R_c, M_c and a_c as regular asymptotic series in powers of $C_r \ll 1$ in the forms

$$\begin{aligned} R_c &= R_0 + R_1 C_r + O(C_r^2), \\ M_c &= M_0 + M_1 C_r + O(C_r^2), \\ a_c &= a_0 + a_1 C_r + O(C_r^2). \end{aligned}$$

Clearly this expansion scheme will fail in the region $a \ll 1$ where the problem is singular but is valid away from $a = 0$ where it is regular. The leading order terms R_0, M_0 and a_0 are just the solutions of the problem when $C_r = 0$ discussed in section 5.1, while the values of the first order terms were obtained numerically by computing R_c, M_c and a_c for a range of values of $C_r \ll 1$ and then evaluating

$$R_1 = \lim_{C_r \to 0} \frac{R_c - R_0}{C_r}, \quad M_1 = \lim_{C_r \to 0} \frac{M_c - M_0}{C_r}, \quad a_1 = \lim_{C_r \to 0} \frac{a_c - a_0}{C_r}.$$

The leading order terms are independent of B_o and, as Davis & Homsy [11] observed, the values of R_1 and M_1 when $B_o \neq 0$ can be calculated by multiplying their values when $B_o = 0$ by the factor $a_0^2/(a_0^2 + B_o)$. Since pure buoyancy-driven convection is independent of C_r the values of R_1 and a_1 at $M = 0$ and M_1 and a_1 at $R = R_c$ are all zero.

Table 3 contains the numerically calculated values of a_0, a_1, R_0 and R_1 in the case $Q = 0$, $B_o = 0$ and $N_u = 0$ and compares them with the corresponding values obtained by Davis & Homsy [11], who used a different method and computed the solutions to the leading and first order problems separately. (Davis & Homsy [11] did not calculate a_1.) The quantities R_1 and a_1 are plotted as functions of M in Fig. 7(a) and Fig. 7(b) respectively,

Table 3. Numerically calculated values of a_0, a_1, R_0 and R_1 in the case $Q=0$, $B_o=0$, $N_u=0$. The quantities a_0^*, R_0^* and R_1^* denote the corresponding values of a_0, R_0 and R_1 calculated by Davis & Homsy [11]. Presumably the value of R_0^* at $M=30$ should be 430 rather than 420.

M	a_0	a_0^*	a_1	R_0	R_0^*	R_1	R_1^*
0	2.0856	2.10	0	668.9982	669	0	0
5	2.0733	2.10	6.5	630.2187	630	2413	2254
10	2.0619	2.08	11.9	590.9898	591	4543	4269
15	2.0515	2.08	16.2	551.3167	551	6358	5917
20	2.0419	2.06	19.2	511.2042	511	7828	7326
25	2.0332	2.06	21.0	470.6562	471	8925	8242
30	2.0254	2.04	21.5	429.6762	420	9619	8914
35	2.0185	2.04	20.8	388.2672	388	9886	9023
40	2.0123	2.04	18.7	346.4314	346	9700	8709
45	2.0071	2.02	15.4	304.1702	304	9039	8092
50	2.0026	2.02	10.8	261.4847	261	7882	6856
55	1.9990	2.02	4.9	218.3751	218	6210	5203
60	1.9962	2.02	-2.4	174.8410	175	4006	3173
65	1.9941	2.02	-11.0	130.8811	131	1256	940
70	1.9929	2.02	-21.0	86.4937	86.5	-2053	-915
75	1.9925	2.02	-32.3	41.6760	41.7	-5931	-904

and the former also shows Davis & Homsy's [11] values of R_1. Fig. 7(c) and Fig. 7(d) show M_1 and a_1 plotted as functions of R. There is evidently broad qualitative agreement but quantitative disagreement between the two sets of data for R_1 [1]. However, both results clearly show that flows dominated by buoyancy effects are *stabilised* by allowing the surface to deform while flows dominated by thermocapillary effects are *destabilised*. Figures 7(b) and 7(d) both show that allowing the surface to deform means that in flows dominated by buoyancy the critical wave number *increases*, while in flows dominated by thermocapillary it *decreases*. These findings agree with the work of Scriven & Sterling [5] and Smith [6] who found that allowing the free surface to deform slightly caused an increase in the critical wave number and a stabilisation of purely buoyancy-driven flows and the work of Takashima [7] and Wilson [24] who found that it caused a decrease in the critical wave number and a destabilisation of purely thermocapillary-driven flows. In the case $Q=0$, $B_o=0$, $N_u=0$ the value of M at which $R_1=0$ is $M\approx 67$ while the value of R at which $M_1=0$ is $R\approx 113$. The values of M and R at which $a_1=0$ are $M\approx 58$ and $R\approx 191$. Notice that the value of R for which $M_1=0$ is not necessarily the same as that for which $a_1=0$ and similarly the value of M for which $R_1=0$ is not necessarily the same as that for which $a_1=0$ and so we must use phrases like "dominated by buoyancy" with care in this context. Figures 8(a), 8(b) show M_1/N_u and a_1 plotted as functions of R in the limiting case $Q=0$, $B_o=0$ and $N_u\to\infty$ and demonstrate the same general trends as in the case $N_u=0$. In this case the value of R at which $M_1=0$ is $R\approx 59$ and $a_1=0$ at $R\approx 112$.

We can perform similar calculations when $Q\neq 0$ and Figs 9(a), 9(b) show M_1 and a_1 plotted as functions of R^* for a range of values of Q in the case $B_o=0$ and $N_u=0$ and demonstrate the same general trends as when $Q=0$. Evidently, the effect of increasing Q is to exaggerate the effect of non-zero C_r. Typical values of R^* at which $M_1=0$ and $a_1=0$ are shown in Table 4 and exhibit no obvious uniform trends as Q increases from zero.

[1] Velarde & Castillo [25] have detected a similar error in another of Davis & Homsy's [11] numerical calculations.

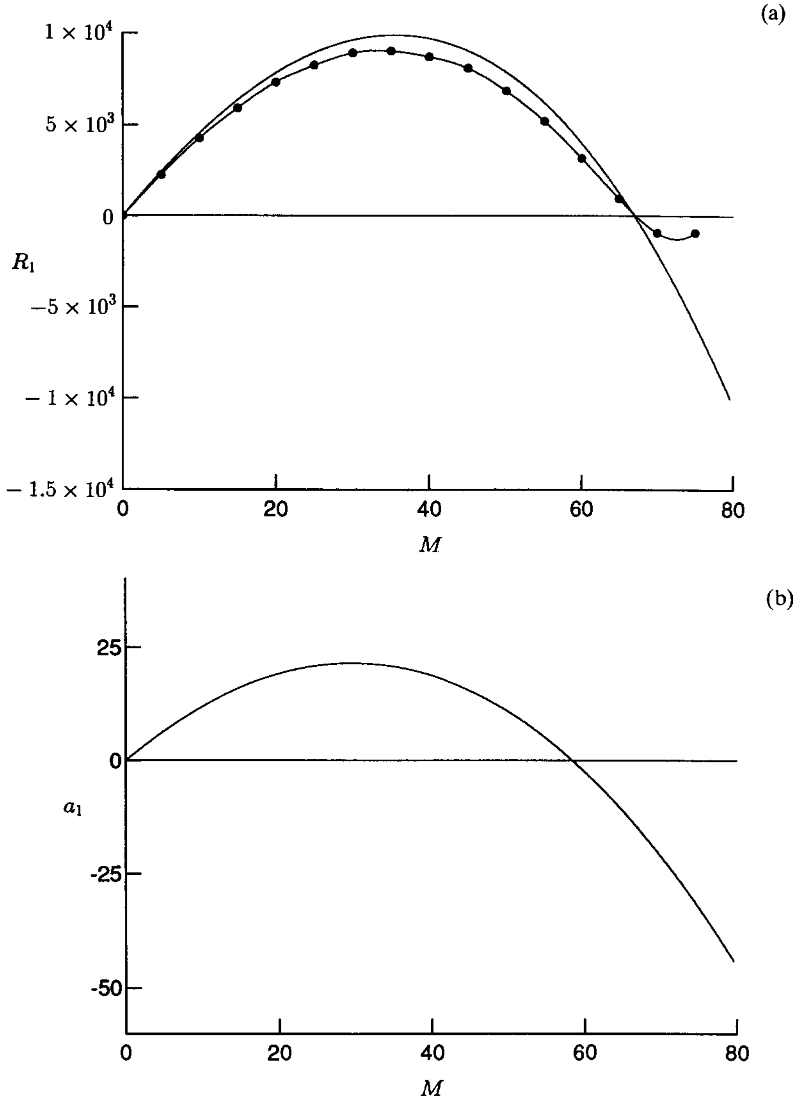

Fig. 7. Numerically calculated values of (a) R_1 and (b) the corresponding value of a_1 plotted as functions of M together with (c) M_1 and (d) the corresponding value of a_1 plotted as functions of R in the case $Q = 0$, $B_o = 0$ and $N_u = 0$. In (a) the dots (•) indicate the corresponding results obtained by Davis & Homsy [11] which are also listed in Table 3.

Table 4. Numerically calculated values of R^* at which $M_1 = 0$ and $a_1 = 0$ respectively for a range of values of Q in the case $B_o = 0$ and $N_u = 0$.

Q	$R^*(M_1 = 0)$	$R^*(a_1 = 0)$
0	0.169	0.285
1	0.167	0.281
10	0.154	0.258
10^2	0.132	0.220
10^3	0.134	0.212
10^4	0.149	0.221

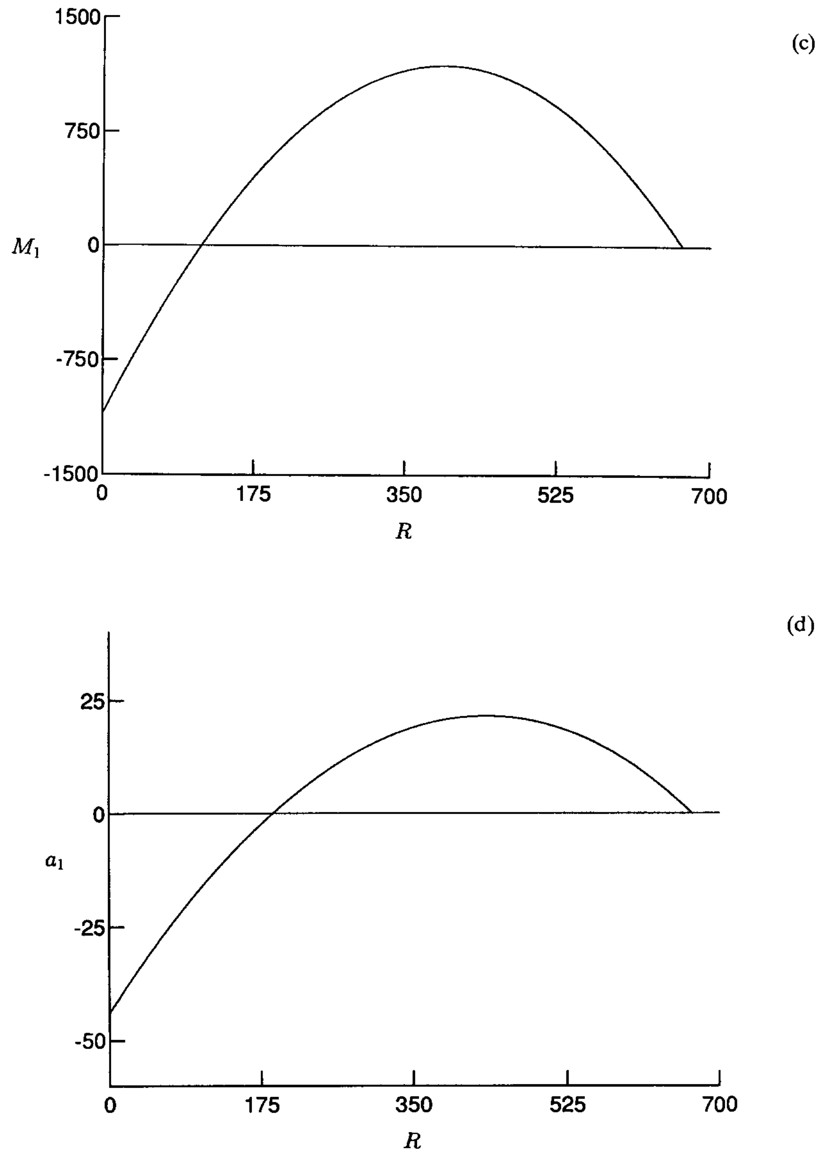

Fig. 7. (c), (d).

5.2.1. Evaluation of M_c

(a) $B_o = 0$

If $C_r \neq 0$ and $B_o = 0$ then $M = O(a^2)$ when $a \ll 1$ and the marginal stability curves attain their minimum value of zero at $a = 0$ so that $M_c = 0$ and $a_c = 0$ for all values of Q. Hence for all values of $M > 0$ disturbances with sufficiently small wave number will be unstable regardless of the value of R.

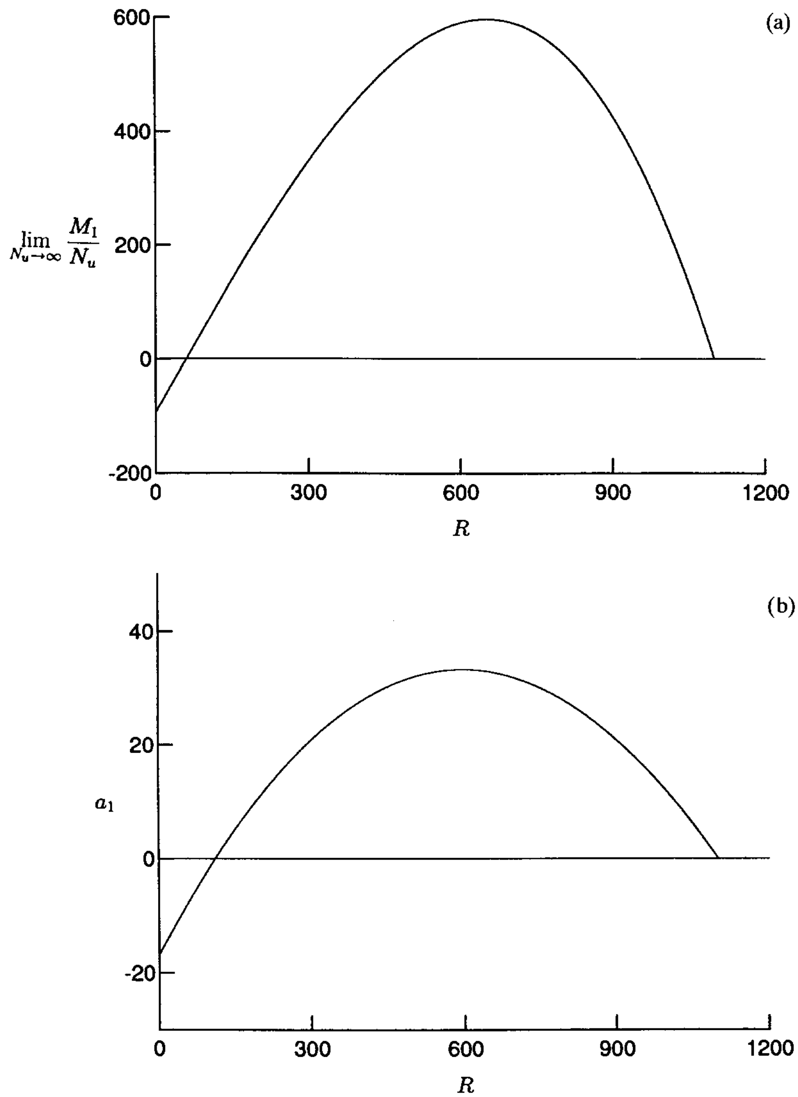

Fig. 8. Numerically calculated values of (a) $\lim_{N_u \to \infty} M_1/N_u$ and (b) the corresponding value of a_1 plotted as functions of R in the case $Q = 0$, $B_o = 0$ and $N_u \to \infty$.

(b) $B_o \neq 0$

If $C_r \neq 0$ and $B_o \neq 0$ then $M = (B_o/C_r)g(Q^{1/2})(1+N_u)$ at $a = 0$ and the marginal stability curves may have a local minimum at $a = 0$. The marginal stability curves can also have a local minimum at a non-zero value of a and so, depending on the absolute values of these local minima, M_c may occur either at $a_c = 0$ or a non-zero value of a_c. Typically M_c and $a_c \neq 0$ increase monotonically as Q is increased from zero until eventually M_c equals the value of M at $a = 0$, which then becomes the global minimum. The critical wave number a_c jumps discontinuously from a non-zero value to zero and thereafter $M_c = (B_o/C_r)g(Q^{1/2})(1 + N_u)$ at $a_c = 0$. Since $g(Q^{1/2}) \to 1$ as $Q \to \infty$, ultimately $M_c \to (B_o/C_r)(1 + N_u)$ as $Q \to \infty$ at

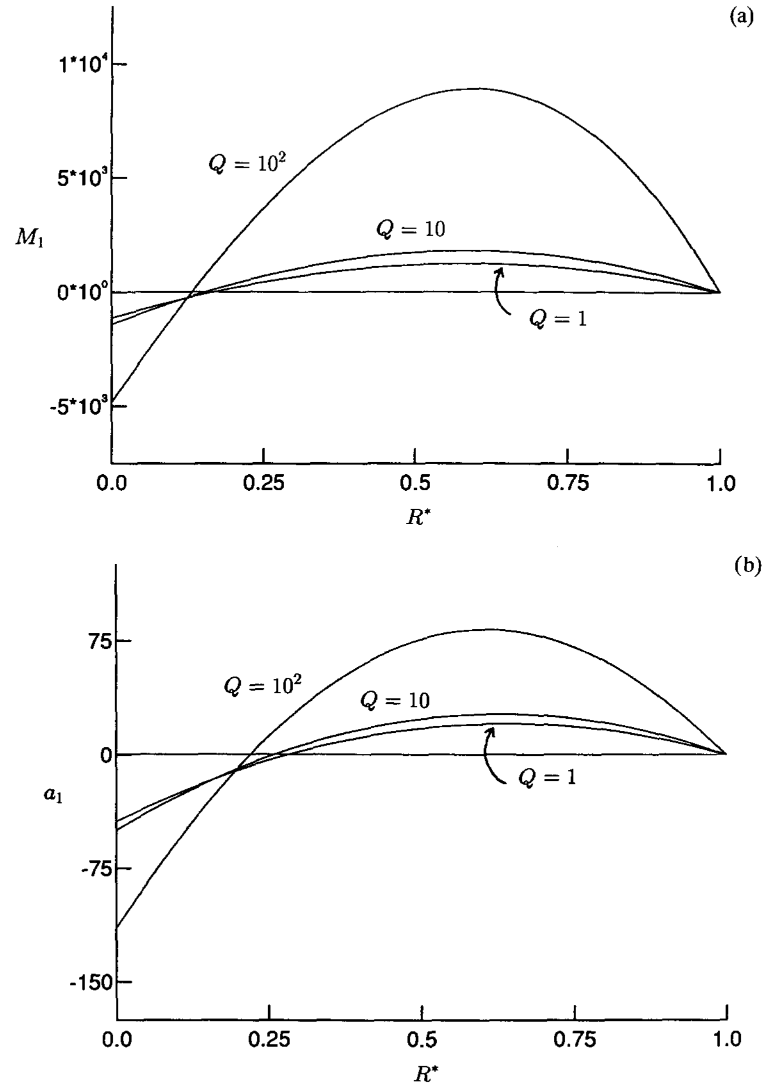

Fig. 9. Numerically calculated values of (a) M_1 and (b) the corresponding value of a_1 plotted as functions of R^* in the case $B_o = 0$ and $N_u = 0$ for $Q = 1$, 10 and 10^2.

$a_c = 0$. The effect of increasing Q is always to stabilise the flow but for Marangoni numbers

$$M > \frac{B_o}{C_r}(1 + N_u)$$

disturbances with sufficiently small wave number will always be unstable no matter how large Q becomes regardless of the value of R. This argument is exactly the same as that given by Wilson [24] in the case $R = 0$.

Figure 10 shows M_c and a_c plotted as functions of R in the case $Q = 0$, $B_o = 1$ and $N_u = 0$ for a range of values of C_r and shows the dramatic effect of the jump in the position of the global minimum of the marginal stability curve as C_r is increased from zero. Figure 11

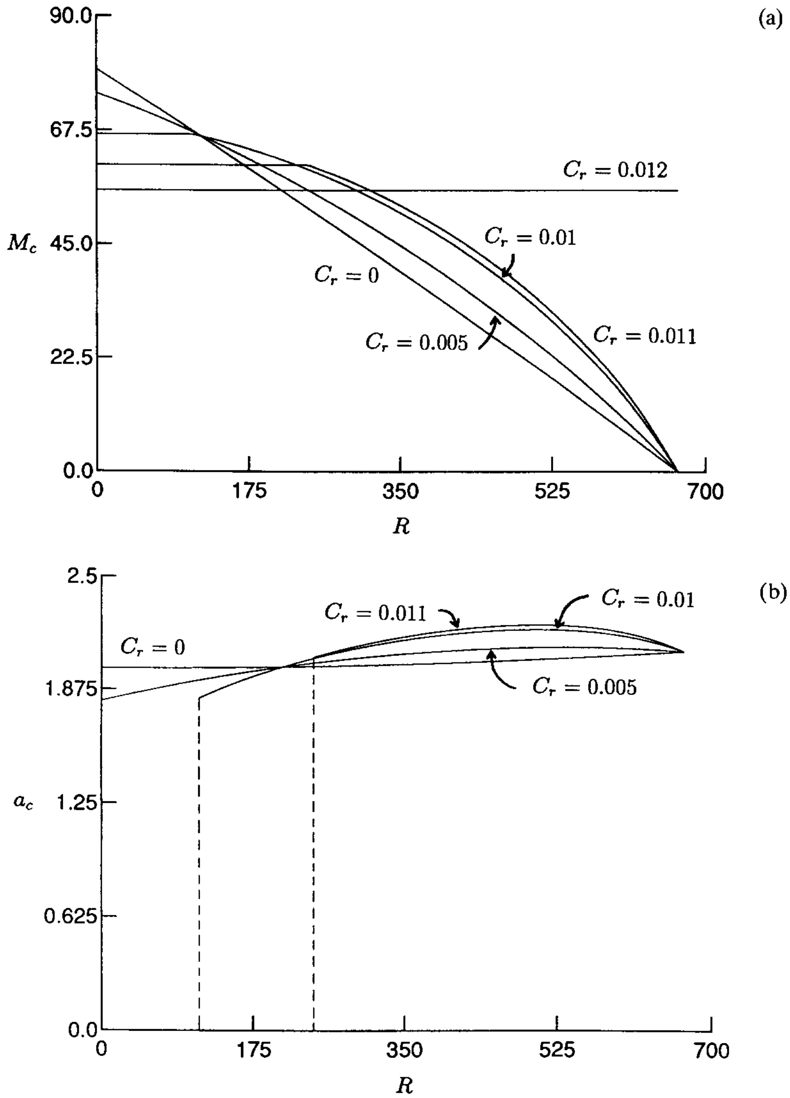

Fig. 10. Numerically calculated values of (a) M_c and (b) a_c in the case $Q = 0$, $B_o = 1$, $N_u = 0$ plotted as functions of R for a range of values of C_r. Notice that the value of a_c jumps discontinuously to zero as R is increased and is identically zero when $C_r = 0.012$.

shows typical values of M_c and a_c plotted as functions of Q in the case $R = 300$, $B_o = 1$ and $N_u = 0$ for different values of C_r and clearly demonstrates the limiting behaviour of M_c as $Q \to \infty$. Figure 12 shows typical values of M_c and a_c plotted as functions of C_r in the case $R = 300$, $B_o = 1$ and $N_u = 0$ for different values of Q. Notice how in the case $Q = 1$ both M_c and a_c are increasing functions of C_r because the flow is dominated by buoyancy effects, while in the cases $Q = 10^2$ and 10^4 both M_c and a_c are decreasing functions of C_r because the flow is dominated by thermocapillary effects. Wilson [24] gives the corresponding results when $R = 0$.

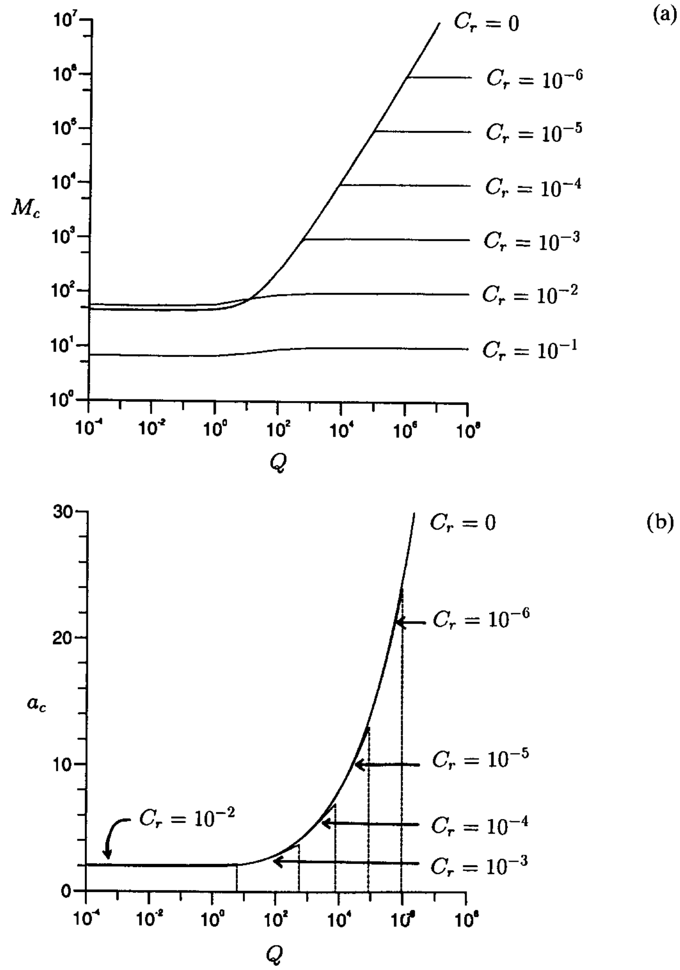

Fig. 11. Numerically calculated values of (a) M_c and (b) a_c in the case $R = 300$, $B_o = 1$, $N_u = 0$ plotted as functions of Q for a range of values of C_r. Notice that the value of a_c jumps discontinuously to zero as Q is increased and is identically zero when $C_r = 10^{-1}$.

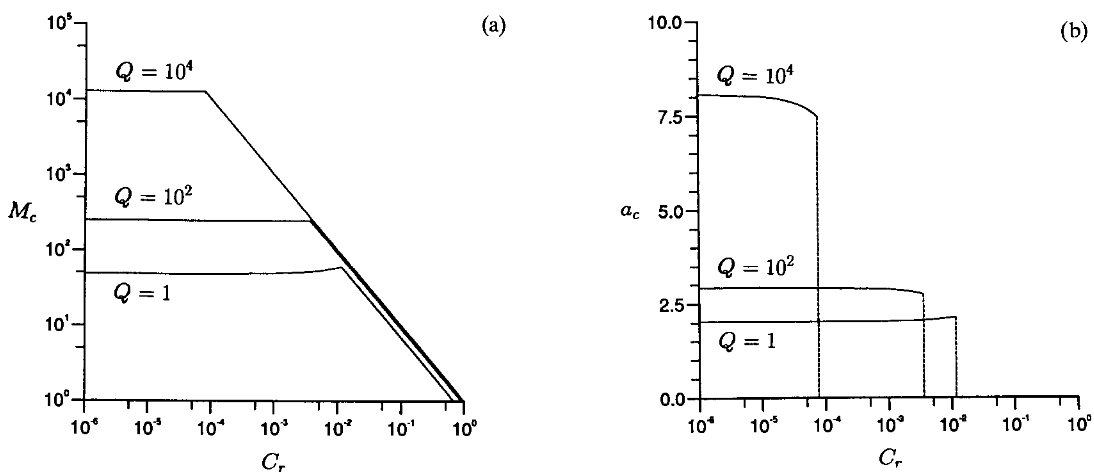

Fig. 12. Numerically calculated values of (a) M_c and (b) a_c in the case $R = 300$, $B_o = 1$, $N_u = 0$ plotted as functions of C_r for a range of values of Q.

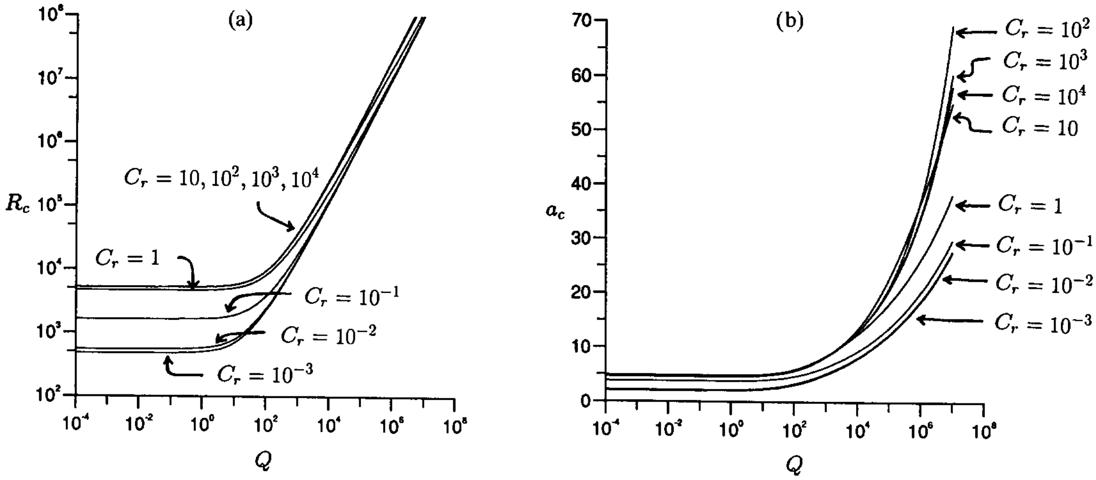

Fig. 13. Numerically calculated values of (a) R_c and (b) a_c in the case $M = 25$, $B_o = 1$, $N_u = 0$ plotted as functions of Q for a range of values of C_r.

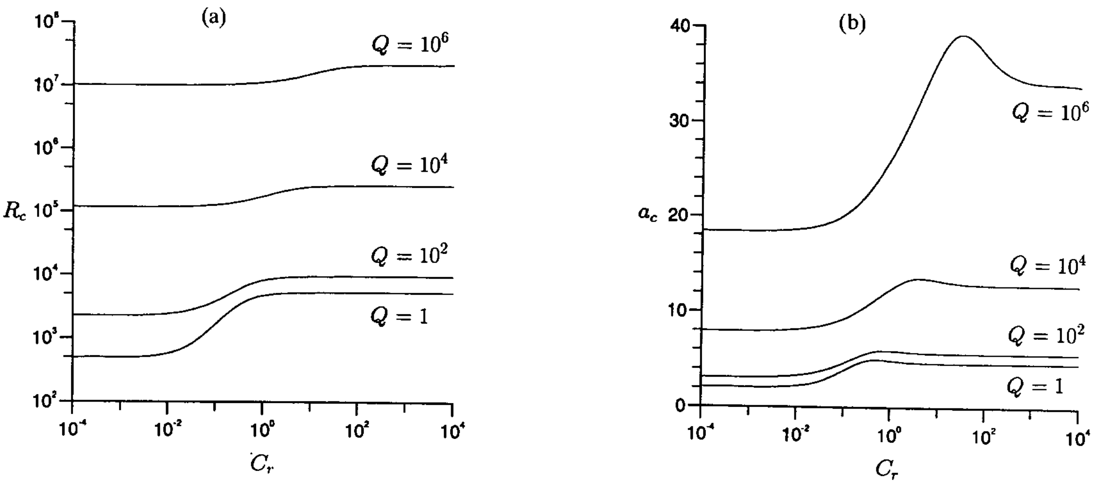

Fig. 14. Numerically calculated values of (a) R_c and (b) a_c in the case $M = 25$, $B_o = 1$, $N_u = 0$ plotted as functions of C_r for a range of values of Q.

5.2.2. *Evaluation of R_c*

We can, of course, regard R rather than M as the critical parameter. Figure 13 shows typical values of R_c and a_c plotted as functions of Q in the case $M = 25$, $B_o = 1$ and $N_u = 0$ for different values of C_r and shows that they only differ significantly from those when $C_r = 0$ for unrealistically large values of C_r. Figure 13 also shows that in the limit $Q \to \infty$ we eventually recover the limiting values for pure buoyancy convection given by equations (27) and (28). Figure 14 shows typical values of R_c and a_c plotted as functions of C_r in the case $M = 25$, $B_o = 1$ and $N_u = 0$ for different values of Q and clearly shows the existence of finite limiting values for both R_c and a_c in the asymptotic limit $C_r \to \infty$.

6. Conclusions

In this paper we have used a combination of analytical and numerical techniques to analyse the effect of a uniform vertical magnetic field on the onset of steady Bénard-Marangoni convection in a horizontal layer of quiescent, electrically conducting fluid subject to a uniform vertical temperature gradient. We have shown that the parameters C_r and B_o are critically important to the onset of steady convection and, in particular, we have clarified the behaviour of the critical parameters R_c, M_c and a_c in the two different limiting cases $C_r \to 0$ and $Q \to \infty$.

Appendix A

In this appendix we analyse the behaviour of the marginal stability curves for the onset of steady convection in the (a, M) plane in the limit of large wave number $a \to \infty$.

If $Q \neq 0$ then in the limit $a \to \infty$ with all the other parameters in the problem apart from M fixed the roots of equation (15) have the asymptotic forms $\xi = \pm\xi_1$, $\pm\xi_2$ and $\pm\xi_3$ where

$$\xi_1 = a + \frac{Q^{1/2}}{2} + \frac{1}{2a}\left(c_2 - \frac{Q}{4}\right) + \frac{1}{2a^2}\left(c_3 + \frac{Q^{3/2}}{8} - \frac{Q^{1/2}c_2}{2}\right) + O\left(\frac{1}{a^3}\right),$$

$$\xi_2 = a - \frac{Q^{1/2}}{2} + \frac{1}{2a}\left(c_2 - \frac{Q}{4}\right) - \frac{1}{2a^2}\left(c_3 + \frac{Q^{3/2}}{8} - \frac{Q^{1/2}c_2}{2}\right) + O\left(\frac{1}{a^3}\right),$$

$$\xi_3 = a + \frac{R}{2aQ} + O\left(\frac{1}{a^3}\right),$$

where we have defined the expressions

$$c_2 = \frac{1}{2}\left(Q - \frac{R}{Q}\right), \quad c_3 = \frac{1}{8Q^{1/2}}\left(Q - \frac{R}{Q}\right)\left(Q + \frac{3R}{Q}\right).$$

The leading order terms in the asymptotic expansions of $A_i = -(\xi_i^2 - a^2)$ and the products $\xi_i A_i$ and $\xi_i^2 A_i$ for $i = 1, 2, 3$ are therefore

$$A_1 = -\left[Q^{1/2}a + c_2 + \frac{c_3}{a}\right] + O\left(\frac{1}{a^2}\right),$$

$$A_2 = -\left[-Q^{1/2}a + c_2 - \frac{c_3}{a}\right] + O\left(\frac{1}{a^2}\right),$$

$$A_3 = -\frac{R}{Q} + O\left(\frac{1}{a^2}\right),$$

together with

$$\xi_1 A_1 = -\left[Q^{1/2}a^2 + \left(c_2 + \frac{Q}{2}\right)a + \left(c_3 + Q^{1/2}c_2 - \frac{Q^{3/2}}{8}\right)\right] + O\left(\frac{1}{a}\right),$$

$$\xi_2 A_2 = -\left[-Q^{1/2}a^2 + \left(c_2 + \frac{Q}{2}\right)a - \left(c_3 + Q^{1/2}c_2 - \frac{Q^{3/2}}{8}\right)\right] + O\left(\frac{1}{a}\right),$$

$$\xi_3 A_3 = -\frac{Ra}{Q} + O\left(\frac{1}{a}\right),$$

and

$$\xi_1^2 A_1 = -\left[Q^{1/2}a^3 + (c_2+Q)\,a^2 + \left(c_3 + 2c_2 Q^{1/2}\right)a\right] + O(1),$$

$$\xi_2^2 A_2 = -\left[-Q^{1/2}a^3 + (c_2+Q)\,a^2 - \left(c_3 + 2c_2 Q^{1/2}\right)a\right] + O(1),$$

$$\xi_3^2 A_3 = -\frac{Ra^2}{Q} + O(1).$$

Using these expressions we can evaluate the determinants D_1 and D_2 to yield $D_1 = 2a^6Q^3 + O(a^5)$ and $D_2 = -a^4Q^3/4 + O(a^3)$ and so the asymptotic expansion of $M = -D_1/D_2$ as $a \to \infty$ is

$$M = 8a^2 + O(a).$$

In the special case of no magnetic field ($Q = 0$) we can follow a similar expansion procedure and obtain the same leading order result.

Appendix B

In this appendix we analyse the marginal stability curves for steady buoyancy-driven convection in the limit of a strong magnetic field, $Q \to \infty$, and obtain asymptotic expressions for R, and hence R_c and a_c, which are in excellent agreement with the numerical results.

Without loss of generality we can set $C_r = 0$. Motivated by the numerical results when $Q \to \infty$ we seek a solution in which $R = O(Q)$ and $a = O(Q^{1/6})$ by writing

$$R = R_1 Q + R_2 Q^{2/3} + o\left(Q^{2/3}\right), \quad a = \hat{a}Q^{1/6} + o\left(Q^{1/6}\right),$$

where the coefficients R_1, R_2 and $\hat{a}$ are to be determined. The roots of equation (15) are then $\xi = \pm\xi_1$, $\pm\xi_2$ and $\pm\xi_3$ where the quantities ξ_1, ξ_2 and ξ_3 have the asymptotic forms

$$\xi_1 = Q^{1/2} + \hat{a}^2 Q^{-1/6} + o\left(Q^{-1/6}\right),$$

$$\xi_2 = \hat{a}Q^{1/6} + \frac{R_1}{2\hat{a}}Q^{-1/6} + \left(\frac{R_2}{2\hat{a}} - \frac{5R_1^2}{8\hat{a}^3}\right)Q^{-1/2} + o\left(Q^{-1/2}\right),$$

$$\xi_3 = iR_1^{1/2}\left[1 - \frac{1}{2R_1}\left(\frac{R_1^2}{\hat{a}^2} + \hat{a}^4 - R_2\right)Q^{-1/3} + o\left(Q^{-1/3}\right)\right],$$

as $Q \to \infty$. The leading order terms in the asymptotic expansions of $A_i = -(\xi_i^2 - a^2)$ and the products $\xi_i A_i$ and $\xi_i^2 A_i$ for $i = 1,2,3$ are therefore

$$A_1 = -\left[Q + \hat{a}^2 Q^{1/3}\right] + o\left(Q^{1/3}\right),$$

$$A_2 = -\left[R_1 + \left(R_2 - \frac{R_1^2}{\hat{a}^2}\right)Q^{-1/3}\right] + o\left(Q^{-1/3}\right),$$

$$A_3 = \hat{a}^2 Q^{1/3} + R_1 - \left(\frac{R_1^2}{\hat{a}^2} + \hat{a}^4 - R_2\right) Q^{-1/3} + o\left(Q^{-1/3}\right),$$

together with

$$\xi_1 A_1 = -\left[Q^{3/2} + 2\hat{a}^2 Q^{5/6}\right] + o\left(Q^{5/6}\right),$$

$$\xi_2 A_2 = -\left[\hat{a}R_1 Q^{1/6} + \left(\hat{a}R_2 - \frac{R_1^2}{2\hat{a}}\right) Q^{-1/6}\right] + o\left(Q^{-1/6}\right),$$

$$\xi_3 A_3 = iR_1^{1/2}\left[\hat{a}^2 Q^{1/3} + \frac{1}{2R_1}\left(R_1^2 - \hat{a}^6 + \hat{a}^2 R_2\right)\right] + o\left(1\right),$$

and

$$\xi_1^2 A_1 = -\left[Q^2 + 3\hat{a}^2 Q^{4/3}\right] + o\left(Q^{4/3}\right),$$

$$\xi_2^2 A_2 = -\left[\hat{a}^2 R_1 Q^{1/3} + \hat{a}^2 R_2\right] + o\left(1\right),$$

$$\xi_3^2 A_3 = -\hat{a}^2 R_1 Q^{1/3} + \hat{a}^2(\hat{a}^4 - R_2) + o\left(1\right).$$

Using these expressions we can evaluate the determinant D_1 and the leading order term in the asymptotic expansion of the equation $D_1 = 0$ is just

$$\sin R_1^{1/2} = 0$$

with the appropriate solution $R_1 = \pi^2$ and the first order term is

$$R_1^2 + \hat{a}^6 - \hat{a}^2 R_2 = 0$$

and so $R_2 = (\pi^4 + \hat{a}^6)/\hat{a}^2$. The leading order terms in the asymptotic expansion of R are therefore

$$R = \pi^2 Q + \frac{\pi^4 + \hat{a}^6}{\hat{a}^2} Q^{2/3} + o\left(Q^{2/3}\right).$$

The critical wave number a_c is determined by solving the equation $\mathrm{d}R/\mathrm{d}a = 0$ at $a = a_c$ which yields no information at leading order, but at first order we obtain $2\hat{a}^6 = R_1^2$ so that $\hat{a} = (\pi^4/2)^{1/6}$ and hence

$$a_c = \left(\frac{\pi^4}{2}\right)^{1/6} Q^{1/6} + o\left(Q^{1/6}\right).$$

Substituting the expression for $\hat{a}$ into the equation for R we obtain

$$R_c = \pi^2 Q + 3\left(\frac{\pi^4}{2}\right)^{2/3} Q^{2/3} + o\left(Q^{2/3}\right).$$

Note that the values of R_1, R_2 and $\hat{a}$, and hence R_c and a_c, are independent of N_u. Chandrasekhar [14, Chap. IV] obtained the same values of R_1, R_2 and $\hat{a}$ in the special case $C_r = 0$, $N_u = \infty$ for a similar problem with two free boundaries for which an explicit solution for R can easily be obtained, and then went on to justify physically why the same limiting behaviour should also occur in geometries with one or two solid boundaries. Subsequently Maekawa & Tanasawa [17] showed numerically, but did not prove, that the limiting values of R_c and a_c were independent of N_u.

Appendix C

In this appendix we extend the method used by Wilson [24] to analyse the marginal stability curves for steady thermocapillary-driven convection in the limit of a strong magnetic field, $Q \to \infty$, when $C_r = 0$ and obtain asymptotic expressions for M, and hence M_c and a_c, which are in excellent agreement with the numerical results.

Motivated by the numerical results when $Q \to \infty$ we seek a solution in which $a = O(Q^{1/4})$ by writing $a = \hat{a}Q^{1/4} + o(Q^{1/4})$ where the coefficient $\hat{a}$ is to be determined. The roots of equation (15) are then $\xi = \pm\xi_1$, $\pm\xi_2$ and $\pm a$ where the quantities ξ_1 and ξ_2 have the asymptotic forms $\xi_1 = Q^{1/2} + \hat{a}^2 + o(1)$ and $\xi_2 = \hat{a}^2 + o(1)$ as $Q \to \infty$. The leading order terms in the asymptotic expansions of $A_i = -(\xi_i^2 - a^2)$ and the products $\xi_i A_i$ and $\xi_i^2 A_i$ for $i = 1, 2$ are therefore

$$A_1 = -\left[Q + \hat{a}^2 Q^{1/2}\right] + o\left(Q^{1/2}\right),$$

$$A_2 = \hat{a}^2 Q^{1/2} + o\left(Q^{1/2}\right),$$

together with

$$\xi_1 A_1 = -\left[Q^{3/2} + 2\hat{a}^2 Q\right] + o\left(Q\right),$$

$$\xi_2 A_2 = \hat{a}^4 Q^{1/2} + o\left(Q^{1/2}\right),$$

and

$$\xi_1^2 A_1 = -\left[Q^2 + 3\hat{a}^2 Q^{3/2}\right] + o\left(Q^{3/2}\right),$$

$$\xi_2^2 A_2 = \hat{a}^6 Q^{1/2} + o\left(Q^{1/2}\right),$$

while $A_3 = 0$. Provided that $N_u \ll Q^{1/4}$ as $Q \to \infty$ we can use these expressions to evaluate the determinants D_1 and D_2 to obtain

$$D_1 = \hat{a}^5 Q^{19/4}(1 - e^{-2\hat{a}^2})\left[1 + \frac{N_u}{\hat{a}Q^{1/4}}\right] + o\left(Q^{9/2}\right),$$

$$D_2 = -\hat{a}^5 Q^{15/4}(1 - e^{-2\hat{a}^2})\left[1 - \frac{2\hat{a}}{\left(1 - e^{-2\hat{a}^2}\right)Q^{1/4}}\right] + o\left(Q^{7/2}\right),$$

and the expansion for $M = -D_1/D_2$ is therefore

$$M = Q + f_1(\hat{a})Q^{3/4} + o\left(Q^{3/4}\right),$$

where we have defined the function

$$f_1(\hat{a}) = \frac{2\hat{a}}{\left(1 - e^{-2\hat{a}^2}\right)} + \frac{N_u}{\hat{a}}.$$

The critical wave number a_c is determined by solving the equation $dM/da = 0$ at $a = a_c$ which yields no information at leading order, but at first order we obtain the equation $df_1/d\hat{a} = 0$;

$$2\hat{a}^2\left[1-e^{-2\hat{a}^2}(1+4\hat{a}^2)\right]-N_u(1-e^{-2\hat{a}^2})^2=0.$$

This equation can easily be solved numerically and values of $\hat{a}$ and $f_1(\hat{a})$ are given in Table 2 for a range of values of N_u. Notice that as $N_u \to \infty$ then $\hat{a} \sim (N_u/2)^{1/2}$ and $f_1(\hat{a}) \sim 2(2N_u)^{1/2}$ as expected, while in the special case $N_u = 0$ we recover the results previously obtained by Wilson [24].

References

1. Lord Rayleigh, On the convection currents in a horizontal layer of fluid when the higher temperature is on the under side. *Phil. Mag.* 32 (1916) : 529-546.
2. A. Pellew, and R.V. Southwell, On maintained convective motion in a fluid heated from below. *Proc. Roy. Soc. (London) A* 176 (1940) : 312-343.
3. R.D. Benguria, and M.C. Depassier, Oscillatory instabilities in the Rayleigh-Bénard problem with a free surface *Phys. Fluids* 30 (6) (1987) : 1678-1682.
4. J.R.A. Pearson, On convection cells induced by surface tension. *J. Fluid Mech.* 4 (1958) : 489-500.
5. L.E. Scriven, and C.V. Sterling, On cellular convection driven by surface-tension gradients : effects of mean surface tension and surface viscosity. *J. Fluid Mech.* 19 (1964) : 321-340.
6. K.A. Smith, On convective instability induced by surface-tension gradients. *J. Fluid Mech.* 24 (2) (1966) : 401-414.
7. M. Takashima, Surface tension driven instability in a horizontal liquid layer with a deformable free surface. I. Steady Convection. *J. Phys. Soc. Japan* 50 (8) (1981) : 2745-2750.
8. M. Takashima, Nature of the Neutral State in Convective Instability Induced by Surface Tension and Buoyancy. *J. Phys. Soc. Japan* 28 (1970) : 810.
9. M. Takashima, Surface tension driven instability in a horizontal liquid layer with a deformable free surface. II. Overstability. *J. Phys. Soc. Japan* 50 (8) (1981) : 2751-2756.
10. D.A. Nield, Surface tension and buoyancy effects in cellular convection. *J. Fluid Mech.* 19 (1964) : 341-352.
11. S.H. Davis, and G.M. Homsy, Energy stability theory for free surface problems : buoyancy-thermocapillary layers. *J. Fluid Mech.* 98 (3) (1980) : 527-553.
12. R.D. Benguria, and M.C. Depassier, On the linear stability of Bénard-Marangoni convection. *Phys. Fluids A* 1 (7) (1989) : 1123-1127.
13. G. Gouesbet, J. Maquet, C. Rozé, and R. Darrigo, Surface-tension and coupled buoyancy-driven instability in a horizontal liquid layer. Overstability and exchange of stability. *Phys. Fluids A* 2 (6) (1990) : 903-911.
14. S. Chandrasekhar, *Hydrodynamic and Hydromagnetic Stability.* OUP (1961).
15. D.A. Nield, Surface tension and buoyancy effects in the cellular convection of an electrically conducting liquid in a magnetic field. *Z.A.M.M.* 17 (1966) : 131-139.
16. T. Maekawa, and I. Tanasawa, Effect of magnetic field on onset of Marangoni convection. *Int. J. Heat Mass Transfer* 31 (2) (1988) : 285-293.
17. T. Maekawa, and I. Tanasawa, Effect of magnetic field and buoyancy on onset of Marangoni convection. *Int. J. Heat Mass Transfer* 32 (7) (1989) : 1377-1380.
18. G.S.R. Sarma, Marangoni convection in a fluid layer under the action of a transverse magnetic field. *Space Res.* 19 (1979) : 575-578.
19. G.S.R. Sarma, Marangoni convection in a liquid layer under the simultaneous action of a transverse magnetic field and rotation. *Adv. Space Res.* 1 (1981) : 55-58.
20. G.S.R. Sarma, Bénard-Marangoni instability in a rotating liquid layer subjected to a transverse magnetic field. *Adv. Space Res.* 3 (5) (1983) : 33-36.
21. G.S.R. Sarma, Effects of interfacial curvature and gravity waves on the onset of thermocapillary convective instability in a rotating liquid layer subjected to a transverse magnetic field. *PhysicoChem. Hydrodynam.* 6 (3) (1985) : 283-300.
22. G.S.R. Sarma, Interaction of surface-tension and buoyancy mechanisms in horizontal liquid layers. *J. Thermophysics* 1 (2) (1987) : 129-135.
23. G.S.R. Sarma, Interfacial effects on the onset of convection in horizontal liquid layers. In *"PhysicoChemical Hydrodynamics"*, ed. M.G. Velarde, Plenum Publishing Corporation, (1988). pp 271-289.
24. S.K. Wilson, The Effect of a Uniform Magnetic Field on the Onset of Marangoni Convection in a Layer of Conducting Fluid. To appear in *Q. Jl. Mech. appl. Math.* (1993).
25. M.G. Velarde, and J.L. Castillo, Transport and reactive phenomena leading to interfacial instability. In *"Convective Transport and Instability Phenomena"*, eds. J. Zierep, H. Oertel, Braun Verlag, Karlsruhe, 1982. pp 235-264.